

# **Better Ceramics Through Chemistry V**

Symposium held April 27-May 1, 1992, San Francisco, California, U.S.A.

EDITORS:

**Mark J. Hampden-Smith**

University of New Mexico  
Albuquerque, New Mexico, U.S.A.

**Walter G. Klemperer**

University of Illinois  
Urbana, Illinois, U.S.A.

**C. Jeffrey Brinker**

Sandia National Laboratories  
Albuquerque, New Mexico, U.S.A.



---

MATERIALS RESEARCH SOCIETY  
Pittsburgh, Pennsylvania

# Contents

PREFACE	xv
MATERIALS RESEARCH SOCIETY SYMPOSIUM PROCEEDINGS	xvi
<b>PART I: MOLECULAR ROUTES TO CERAMIC MATERIALS</b>	
*NEW CHEMISTRY FOR THE SOL-GEL PROCESS: ACETONE AS A NEW CONDENSATION REAGENT Subhash C. Goel, Michael Y. Chiang, Patrick C. Gibbons, and William E. Buhro	3
*HETEROMETALLIC AGGREGATES AS INTERMEDIATES ON THE MOLECULAR ROUTES TO MULTICOMPONENT OXIDES Liliane G. Hubert-Pfalzgraf	15
FURTHER STUDIES ON ALUMINUM OXOALKOXIDE CLUSTERS R.A. Sinclair, M.L. Brostrom, W.B. Gleason, and R.A. Newmark	27
STUDIES ON THE FORMATION OF TIN(IV) OXYGEN COMPOUNDS BY SOL-GEL-PROCESS H. Reuter, M. Kremser, D. Schröder, and M. Jansen	33
HYDROLYSIS-CONDENSATION OF ALKYL TIN-TRIALKOXIDES François Ribot, F. Banse, and C. Sanchez	45
HYDROLYSIS AND CONDENSATION OF MODIFIED TIN(IV) ALKOXIDE COMPOUNDS TO FORM CONTROLLED POROSITY MATERIALS Christophe Roger, M.J. Hampden-Smith, and C.J. Brinker	51
POLYNUCLEAR TITANIUM OXOALKOXIDES: MOLECULAR BUILDING BLOCKS FOR NEW MATERIALS? Y.W. Chen, W.G. Klemperer, and C.W. Park	57
RAMAN AND SURFACE ENHANCED RAMAN SPECTROSCOPY OF TITANIUM CARBOXYLATES Beatrice A. Van Vlierberge-Torgerson, Dilum Dunuwila, and Kris A. Berglund	65
HYDROLYSIS OF ZIRCONIUM PROPOXIDE BY AN ESTERIFICATION REACTION I. Laaziz, A. Larbot, C. Guizard, A. Julbe, and L. Cot	71
MOLECULAR DESIGN OF CARBOXYLIC PRECURSORS FOR ZIRCONIA Allen W. Apblett, Jin Lei, and Galina D. Georgeva	77
PROPERTIES OF ZrO <sub>2</sub> GELS PREPARED BY CONTROLLED CHEMICAL MODIFICATION METHOD OF ALKOXIDE Hisao Suzuki, Hajime Saito, and Hiroaki Hayashi	83
SINGLE-COMPONENT ROUTES TO PEROVSKITE PHASE MIXED METAL OXIDES Clive D. Chandler, M.J. Hampden-Smith, and C.J. Brinker	89
SYNTHESIS OF BARIUM TITANATE BY A BASIC pH PECHINI PROCESS Suresh Kumar and Gary L. Messing	95

\*Invited Paper

PREPARATION OF STRONTIUM TITANATE POWDERS BY DECOMPOSITION OF POLYMERIC PRECURSORS S.L. Peschke, M. Ciftcioglu, D.H. Doughty, and J.A. Voigt	101
SYNTHESIS, STRUCTURE, AND CHARACTERIZATION OF $\text{La}_{1-x}\text{Ba}_x\text{TiO}_3$ ( $0 \leq x \leq 1$ ) Joseph E. Sunstrom IV and Susan M. Kauzlarich	107
COMBUSTION SYNTHESIS OF Sr-SUBSTITUTE $\text{LaCo}_{0.4}\text{Fe}_{0.6}\text{O}_3$ POWDERS J.J. Kingsley, L.A. Chick, G.W. Coffey, D.E. McCready, and L.R. Pederson	113
SYNTHESIS OF FERROELECTRIC PEROVSKITES THROUGH AQUEOUS SOLUTIONS TECHNIQUES G. Guzmán-Martel, M.A. Aegerter, and P. Barboux	121
NEW GROUP 2 COMPOUNDS USEFUL FOR PREPARATION OF THIN FILMS OF ELECTRONIC CERAMICS William S. Rees, Jr., Kerstin A. Dippel, Michael W. Carris, Celia R. Caballero, Debra A. Moreno, and Werner Hesse	127
STABILIZATION OF METAL ALKOXIDES (M = Ba, Cu) BY ALKANOLAMINES L.G. Hubert-Pfalzgraf, M.C. Massiani, J.C. Daran, and J. Vaissermann	135
SOLID STATE STRUCTURES, DECOMPOSITION PATHWAYS, AND VAPOR PHASE BY-PRODUCTS OF $\text{Y}(\text{acac})_3$ TYPE OMVPE PRECURSORS FOR THIN FILMS OF YTTRIUM-CONTAINING CERAMIC MATERIALS William S. Rees, Jr., Henry A. Luten, Michael W. Carris, Eric J. Duskocil, and Virgil L. Goedken	141
AGGREGATION AND HYDROLYSIS REACTIONS OF BISMUTH ALKOXIDES Kenton H. Whitmire, Carolyn M. Jones, Michael D. Burkart, J. Chris Hutchison, and Andrew L. McKnight	149
SOL-GEL SYNTHESIS OF $\text{YBa}_2\text{Cu}_3\text{O}_{7-x}$ USING YTTRIUM, BARIUM, AND COPPER POLYETHER ALKOXIDE PRECURSORS Catherine J. Page, Carol S. Houk, and Gary A. Burgoine	155
PREPARATION OF BSCCO PRECURSORS BY WATER EXTRACTION VARIANT OF SOL-GEL PROCESS A. Deptuła, W. Łada, T. Olczak, and A. Di Bartolomeo	161
FROM CERAMICS TO SUPERCONDUCTORS: RAPID MATERIALS SYNTHESIS BY SOLID-STATE METATHESIS REACTIONS Randolph E. Treece, Edward G. Gillan, Richard M. Jacobinas, John B. Wiley, and Richard B. Kaner	169
CHARACTERIZATIONS OF SOL-GEL CORDIERITE PRECURSORS Yun Fa Chen, Saïd El Hadigui, and Serge Vilminot	175
SOL-GEL PROCESS FROM HETEROBIMETALLIC ALKOXIDES TO INCORPORATE LANTHANIDES IN AN ALUMINA MATRIX Chaitanya K. Narula	181
SYNTHESIS OF NEW COMPOUNDS BY ION-EXCHANGE REACTIONS M.E. Villafuerte-Castrejón, and A. Aragón-Piña	187

COMPARATIVE STUDY OF THE SOL-GEL AND METALLO-ORGANIC DECOMPOSITION (MOD) PROCESSES FOR THE PREPARATION OF INORGANIC MATERIALS	193
Gustavo R. Paz-Pujalt, W. Nie, and C. Lurin	
<b>PART II: PARTICULATE AND POLYMERIC SOLS</b>	
*COMPLEXATION OF Zr(IV) PRECURSORS IN AQUEOUS SOLUTIONS	201
J. Livage, M. Chatry, M. Henry, and F. Taulelle	
FRACTAL GROWTH DURING GELATION	213
Edward J.A. Pope	
SOLVENT QUALITY EFFECTS IN SOL-GEL PROCESSING	219
Joseph K. Bailey	
A RAMAN SPECTROSCOPIC STUDY OF THE INITIAL STAGES OF HYDROLYSIS OF TETRAETHOXY-SILANE	225
J.D. Barrie and K.A. Aitchison	
SILICON-29 NMR STUDY ON THE INITIAL STAGE OF THE CO-HYDROLYSIS OF TETRAETHOXY-SILANE AND METHYLTRIETHOXY-SILANE	231
Yoshiyuki Sugahara, Yoichi Tanaka, Shuji Sato, Kazuyuki Kuroda, and Chuzo Kato	
STRUCTURAL CHARACTERIZATION OF GELS PREPARED FROM CO-HYDROLYSIS OF TETRAETHOXY-SILANE AND DIMETHYLDIETHOXY-SILANE	237
Florence Babonneau, Laurence Bois, and Jacques Livage	
ELECTRONEGATIVITY-BASED COMPUTATION OF <sup>29</sup> Si CHEMICAL SHIFTS	243
M. Henry, C. Gerardin, and F. Taulelle	
RAMAN AND INFRARED STUDY OF METAL ALKOXIDES DURING SOL-GEL PROCESS	249
O. Poncelet, J-C. Robert, and J. Guilment	
REACTION KINETICS FOR THE HYDROLYSIS OF TITANIUM ISOPROPOXIDE CARBOXYLATE COMPLEXES	257
Charles D. Gagliardi, Dilum Dunuwila, Beatrice A. Van Vlierberge-Torgerson, and Kris A. Berglund	
USAXS AND X-RAY MICROSCOPY INVESTIGATIONS ON SILICA AND PRECURSORS OF ZEOLITES	263
Theo P.M. Beelen, Wim H. Dokter, Harold F. van Garderen, Rutger A. van Santen, Mike T. Browne, and Graeme R. Morrison	
RHEOLOGY OF ZIRCONIA-ALUMINA GELCASTING SLURRIES	269
A. Bleier, O.O. Omatete, and C.G. Westmoreland	
PRODUCTION OF SPHERICAL POWDERS OF INORGANIC COMPOUNDS BY WATER EXTRACTION VARIANT OF SOL-GEL PROCESS	277
A. Deptula, J. Rebandel, W. Drozda, W. Łada, and T. Olczak	
NOVEL PRECIPITATION ROUTE TO SILICA GRAIN	285
Barbara Simms and Tom Gallo	

\*Invited Paper

THEORETICAL AND EXPERIMENTAL INVESTIGATIONS OF THE GROWTH OF SILICA AND TITANIA PARTICLES IN LOW MOLECULAR WEIGHT ALCOHOLS	291
Michael T. Harris, Osman A. Basaran, and Charles H. Byers	
THE FAST SOL-GEL SYNTHETIC ROUTE TO SUPPORTED GLASS FILMS: SYNTHETIC FEATURES, SCOPE, APPLICATIONS AND MECHANISTIC STUDIES	297
Y. Haruvy and S.E. Webber	
STABILITY OF AQUEOUS SUSPENSIONS OF HIGH SURFACE AREA ZIRCONIA POWDERS IN THE PRESENCE OF POLYACRYLIC ACID POLYELECTROLYTE	303
Michel M.R. Boutz, R.J.M. Olde Scholtenhuis, A.J.A. Winnubst, and A.J. Burggraaf	
PRODUCTION OF SOLS FROM AGGREGATED TITANIA PRECIPITATES	309
John R. Bartlett and James L. Woolfrey	
<b>PART III: CERAMIC THIN FILMS, COATINGS, MEMBRANES, AND FIBERS</b>	
*STRESS AND PHASE TRANSFORMATION PHENOMENA IN OXIDE FILMS: REAL-TIME SPECTROSCOPIC MEASUREMENTS	319
Gregory J. Exarhos and Nancy J. Hess	
*CHEMICAL PROCESSING OF FERROELECTRIC NIOBATES EPITAXIAL FILMS	331
Shin-Ichi Hirano, Toshinobu Yogo, Koichi Kikuta, Hisanobu Urahata, Yasuhide Isobe, Toshiyuki Morishita, Koji Ogiso, and Yasuhiro Ito	
*CHEMICAL PROCESSING AND PROPERTIES OF NANOCRYSTALLINE BaTiO <sub>3</sub>	339
Z. Xu, H.K. Chae, M.H. Frey, and D.A. Payne	
OPTIMIZATION OF SOL-GEL DERIVED PZT THIN FILMS BY THE INCORPORATION OF EXCESS PBO	345
G. Teowee, J.M. Boulton, and D.R. Uhlmann	
ELECTRICAL AND OPTICAL PROPERTIES OF SOL-GEL PROCESSED Pb(Zr,Ti)O <sub>3</sub> FILMS	351
S.D. Ramamurthi, S.L. Swartz, K.R. Marken, J.R. Busch, and V.E. Wood	
ELECTRICAL PROPERTIES OF CRYSTALLINE AND AMORPHOUS Pb(Zr <sub>x</sub> Ti <sub>1-x</sub> )O <sub>3</sub> THIN FILMS PREPARED BY THE SOL-GEL TECHNIQUE	359
Yuhuan Xu, Chih-Hsing Cheng, Ren Xu, and John D. Mackenzie	
PREPARATION OF BaTiO <sub>3</sub> AND PbTiO <sub>3</sub> THIN FILMS ON BaPbO <sub>3</sub> SUBSTRATES BY THE SOL-GEL METHOD AND THEIR PROPERTIES	365
M. Kuwabara, T. Kuroda, S. Takahashi, and T. Azuma	
LOW TEMPERATURE FORMATION OF FERROELECTRIC THIN FILMS	371
Chi Kong Kwok and Seshu B. Desu	
MICROSTRUCTURAL VARIATIONS IN SOL-GEL PROCESSED LITHIUM NIOBATE THIN FILMS	377
Vikram Joshi, Grace K. Goo, and Martha L. Mecartney	

\*Invited Paper

THE GROWTH OF SINGLE CRYSTAL-LIKE AND POLYCRYSTAL KNbO <sub>3</sub> FILMS VIA SOL-GEL PROCESS	383
Chih-Hsing Cheng, Yuhuan Xu, John D. Mackenzie, Jie Zhang, and LeRoy Eyring	
PREPARATION AND CHARACTERIZATION OF SOL-GEL THIN FILMS OF KTiOPO <sub>4</sub>	389
Mark A. Harmer and Mark G. Roelofs	
SYNTHESIS OF CUPRATE BASED HIGH-T <sub>c</sub> SUPERCONDUCTORS BY POLYMERIZED COMPLEX METHOD	395
Masato Kakihana, Masahiro Yoshimura, Hiromasa Mazaki, Hiroshi Yasuoka, and Lars Börj Esson	
APPLICATION OF ETHANOLAMINE METHOD FOR THE PREPARATION OF INDIUM OXIDE-BASED SOLS AND FILMS	401
Yasutaka Takahashi, Hideo Hayashi, and Yutaka Ohya	
GROWTH OF ORIENTED TIN OXIDE THIN FILMS FROM AN ORGANOTIN COMPOUND BY SPRAY PYROLYSIS	407
Isao Yagi and Shoji Kaneko	
SOL-GEL MULTILAYERS APPLIED BY A MENISCUS COATING PROCESS	413
Jerald A. Britten and Ian M. Thomas	
PHASE TRANSFORMATIONS IN SOL-GEL YAG FILMS	421
R.S. Hay	
STRUCTURAL AND ELECTRICAL PROPERTIES OF Mn-Co-Ni-O THIN FILMS PREPARED BY DIP-COATING TECHNIQUE	429
Shoji Kaneko, Naoto Mazuka, and Tamotsu Yamada	
MOLECULAR RECOGNITION ON ACOUSTIC WAVE DEVICES: MODIFIED ZEOLITE-SILICA THIN FILMS WITH TAILORED ADSORPTION PROPERTIES	435
Yongan Yan, Thomas Bein, Kelly D. Brown, Ray Forrister, and Jeffrey Brinker	
STRUCTURE OF THIN SOL-GEL COATINGS NEAR THE SURFACE OF SUBSTRATES	443
Hiroshi Hirashima and Takao Kusaka	
LASER DENSIFICATION OF SOL-GEL DERIVED TiO <sub>2</sub> - THIN FILMS	449
N. Arfsten, B. Lintner, M. Heming, O. Anderson, and C.R. Otter-Mann	
*CRYSTALLINE THIN AND/OR THICK FILM OF PEROVSKITE-TYPE OXIDES BY HYDROTHERMAL ELECTROCHEMICAL TECHNIQUES	457
Masahiro Yoshimura	
ELECTROPHORETIC DEPOSITION OF SOL-GEL-DERIVED CERAMIC COATINGS	465
Yining Zhang, C. Jeffrey Brinker, and Richard M. Crooks	
CORROSION RESISTANT ZrO <sub>2</sub> SOL-GEL COATING ON STAINLESS STEEL	471
M. Atik and M.A. Aegerter	
PROTECTIVE ZIRCONIA THIN FILMS ON METAL SUBSTRATES	477
Andrea Tomasi, Paolo Scardi, and Fabio Marchetti	

\*Invited Paper

PLASMA SPRAYED ALUMINA-TITANIA COATINGS T.J. Steeper, A.J. Rotolico, J.E. Nerz, W.L. Riggs II, D.J. Varacalle, Jr., and G.C. Wilson	485
A MICROPOROUS SILICA MEMBRANE Wilhelm F. Maier and Herbert O. Schramm	493
THERMAL STABILITY OF SUPPORTED TITANIA MEMBRANES Krishnankutty-Nair P. Kumar, V.T. Zaspalis, F.F.M. De Mul, Klaas Keizer, and Anthonie J. Burggraaf	499
PREPARATION AND CHARACTERIZATION OF MICROPOROUS SOL-GEL DERIVED CERAMIC MEMBRANES FOR GAS SEPARATION APPLICATIONS R.S.A. De Lange, J.H.A. Hekkink, K. Keizer, and A.J. Burggraaf	505
IMOGOLITE AS A MATERIAL FOR FABRICATION OF INORGANIC MEMBRANES Jeffrey C. Huling, Joseph K. Bailey, Douglas M. Smith, and C. Jeffrey Brinker	511
SOL-GEL DERIVED PZT FIBERS J.M. Boulton, G. Teowee, and D.R. Uhlmann	517
 <b>PART IV: AGING, DRYING, AND CONSOLIDATION OF GELS</b>	
*MECHANICS OF GELS George W. Scherer	527
THE EFFECT OF GEL AGING ON THE PHYSICAL AND OPTICAL PROPERTIES OF A GEL-DERIVED GRIN GLASS Mark A. Banash, Tessie M. Che, J. Brian Caldwell, Robert M. Mininni, Paul R. Soskey, Victor N. Warden, and Hui H. Chin	535
SOL-GEL FILMS WITH TAILORED MICROSTRUCTURES Deborah L. Logan, Carol S. Ashley, and C. Jeffrey Brinker	541
PORE SIZE AND SURFACE TEXTURE MODIFICATION OF SILICA VIA TRIALKYLSILYLATION Duen-Wu Hua and Douglas M. Smith	547
PORE STRUCTURE EVOLUTION OF SILICA GEL DURING AGING/ DRYING: EFFECT OF SURFACE TENSION Ravindra Deshpande, Douglas M. Smith, and C. Jeffrey Brinker	553
INTERPRETATION OF AEROGEL SHRINKAGE DURING DRYING Bharath Rangarajan and Carl T. Lira	559
PREPARATION OF LOW-DENSITY AEROGELS AT AMBIENT PRESSURE Douglas M. Smith, Ravindra Deshpande, and C. Jeffrey Brinker	567
PREPARATION AND PHYSICAL PROPERTIES OF V <sub>2</sub> O <sub>5</sub> AEROGELS Hiroshi Hirashima and Kazumi Sudoh	573

#### **PART V: CERAMIC COMPOSITES**

LEUCITE-POLLUCITE GLASS CERAMICS: A NEW FAMILY OF REFRACTORY MATERIALS WITH ADJUSTABLE THERMAL-EXPANSION R.L. Bedard, R.W. Broach, and E.M. Flanigen	581
--	-----

\*Invited Paper

SINTERING PROCESS AND MECHANICAL PROPERTIES FOR OXIDE-BASED NANOCOMPOSITES	589
Koichi Niihara, Atsushi Nakahira, and Masahiro Inoue	
AMORPHIZATION AT THE METAL-CERAMIC INTERFACE IN Nb—Al <sub>2</sub> O <sub>3</sub> COMPOSITE THROUGH EXTENSIVE INTERPHASE DIFFUSION	595
Abhijit Ray and Shyam K. Samanta	
MODELING AND EXPERIMENTAL INVESTIGATIONS OF PRESSURE INFILTRATION OF SOL-GEL PROCESSED 3-D CERAMIC MATRIX COMPOSITES	601
Hsien-Kuang Liu and Azar Parvizi-Majidi	
<b>PART VI: HYBRID ORGANIC/INORGANIC MATERIALS</b>	
*MACRO-DEFECT-FREE CEMENT: A NOVEL ORGANOCERAMIC COMPOSITE	609
J. Francis Young and M. Berg	
*METAL COMPLEXES IN OXIDIC MATRICES	621
Ulrich Schubert, Boris Breitscheidel, Hermann Buhler, Christian Egger, and Wlodzimierz Urbaniak	
FORMATION OF HIGHLY DISPERSED METALS ON FUNCTIONALIZED SILICA SUPPORTS	633
Francois Rousseau, Z. Duan, M.J. Hampden-Smith, and A. Datye	
ENERGY TRANSFER BETWEEN Eu <sup>2+</sup> , Eu <sup>3+</sup> AND Rh6G IN SILICA, ZIRCONIA AND ALUMINA GELS	639
W. Nie, B. Dunn, C. Sanchez, and P. Griesmar	
DIFFUSION OF CARBON MONOXIDE IN METALORGANIC THIN FILMS DERIVED FROM TITANIUM ALKOXIDE CARBOXYLATES	645
Charles D. Gagliardi, Dilum Dunuwila, C.K. Chang, and Kris A. Berglund	
RIGIDOCROMISM AS A PROBE OF GELATION, AGING, AND DRYING IN SOL-GEL DERIVED ORMOSILS	651
Stephen D. Hanna, Bruce Dunn, and Jeffrey I. Zink	
SYNTHESIS AND CHARACTERIZATION OF ORGANIC DYE DOPED SILICA GLASSES	657
Ilzoo Lee, Josephine Covino, and Michael D. Seltzer	
DENSE XEROGEL MATRICES AND FILMS FOR OPTICAL MEMORY	663
F. Chaput, J.P. Boilot, F. Devreux, M. Canva, P. Georges, and A. Brun	
*TAILORING OF TRANSITION METAL ALKOXIDES VIA COMPLEXATION FOR THE SYNTHESIS OF HYBRID ORGANIC-INORGANIC SOLS AND GELS	669
C. Sanchez, M. In, P. Toledano, and P. Griesmar	
STRUCTURE-RELATED MECHANICAL PROPERTIES OF ORMOSILS BY SOL-GEL PROCESS	681
Yi Hu and John D. Mackenzie	
MONITORING OF HETEROPOLYSILOXANE THIN FILM PROPERTIES USING RHEOLOGICAL AND ACOUSTIC CHARACTERIZATION METHODS	687
C. Guizard, P. Lacan, J.M. Saurel, F. Hajoub, and L. Cot	

\*Invited Paper



THE EFFECT OF ULTRASONIC RADIATION ON GELATION AND PROPERTIES OF ORMOSILS Kazuki Morita, Yi Hu, and John D. Mackenzie	693
PREPARATION OF ARYL-BRIDGED POLYSILSESQUOXANE AEROGELS Douglas A. Loy, Kenneth J. Shea, and Edward M. Russick	699
CHARACTERIZATION OF MICROPOROUS SILICA GELS PREPARED FROM MODIFIED SILICON ALKOXIDES W.G. Fahrenholtz and D.M. Smith	705
HYPERVALENT SILICONATE MATERIALS. SYNTHESIS AND CHARACTERIZATION OF NOVEL LADDER AND NETWORK IONOMERS Kenneth J. Shea, Douglas A. Loy, and James H. Small	711
MULTIFUNCTIONAL (METH) ACRYLATE ALKOXYSILANES A NEW TYPE OF REACTIVE COMPOUNDS H. Wolter, W. Glaubitt, and K. Rose	719
CHARACTERISATION OF HYDROLYSED ALKOXYSILANES AND ZIRCONIUMALKOXIDES FOR THE DEVELOPMENT OF UV-CURABLE SCRATCH RESISTANT COATINGS K. Greiwe, W. Glaubitt, S. Amberg-Schwab, and K. Piana	725
MULTIFUNCTIONAL ACRYLATE ALKOXYSILANES FOR POLYMERIC MATERIALS K. Rose, H. Wolter, and W. Glaubitt	731
<b>PART VII: NOVEL ROUTES TO NON-OXIDE CERAMICS</b>	
*PREPARATION OF NON-OXIDE CERAMICS BY PYROLYSIS OF ORGANOMETALLIC PRECURSORS Leonard V. Interrante, Wayne R. Schmidt, Paul S. Marchetti, and Gary E. Maciel	739
CHEMICALLY DESIGNED, UV CURABLE POLYCARBOSILANE POLYMERS Kevin J. Thorne, Stephen E. Johnson, Haixing Zheng, John D. Mackenzie, and M.F. Hawthorne	749
PROCESSING OF SiC-BASED FIBRES FROM POLYCARBOSILANE Vasilios Kalyvas, J.C. Ko, G.C. East, J.E. McIntyre, B. Rand, and F.L. Riley	755
POLYMER-DERIVED SILICON CARBIDE FIBERS WITH IMPROVED THERMOMECHANICAL STABILITY W. Toreki, C.D. Batich, M.D. Sacks, M. Saleem, and G.J. Choi	761
SYNTHESES, STRUCTURES AND PROPERTIES OF POLYCARBOSILANES FORMED DIRECTLY BY POLYMERIZATION OF ALKENYLSILANES John Masnovi, Xin Y. Bu, Kassahun Beyene, Paula Heimann, Terrence Kacik, A. Harry Andrist, and Frances I. Hurwitz	771
NMR CHARACTERIZATION OF SILICON CARBIDES AND CARBONITRIDES. A METHOD FOR QUANTIFYING THE SILICON SITES AND THE FREE CARBON PHASE C. Gerardin, M. Henry, and F. Taulelle	777

\*Invited Paper

HIGH TEMPERATURE STABILITY OF OXYCARBIDE GLASSES Hanxi Zhang and Carlo G. Pantano	783
SILICON OXYCARBIDE GLASSES FROM SOL-GEL PRECURSORS F. Babonneau, G.D. Soraru, G. D'Andrea, S. Dire, and L. Bois	789
THE ROLE OF Si-H FUNCTIONALITY IN OXYCARBIDE GLASS SYNTHESIS Anant K. Singh and Carlo G. Pantano	795
CHARACTERIZATION OF HIGH SURFACE AREA SILICON OXYNITRIDES Peter W. Lednor, Rene de Ruiter, and Kees A. Emeis	801
ISOCYANATE-MODIFIED POLYSILAZANES: CONVERSION TO CERAMIC MATERIALS Joanne M. Schwark and Mark J. Sullivan	807
REACTION SINTERING MECHANISM OF SUBMICROMETER SILICON POWDER IN NITROGEN Yoshiyuki Yasutomi, Masahisa Sobue, and Jiro Kondo	813
SYNTHESIS OF ADVANCED CERAMICS IN THE SYSTEMS Si-B-N AND Si-B-N-C EMPLOYING NOVEL PRECURSOR COMPOUNDS H.-P. Baldus, O. Wagner, and M. Jansen	821
DESIGN AND SYNTHESIS OF CHEMICAL PRECURSORS TO BORON CARBIDE Xiaoguang Yang, Stephen Johnson, M. Frederick Hawthorne, Haixing Zheng, Kevin Thorne, and J.D. Mackenzie	827
ALKYNYL SUBSTITUTED CARBORANES AS PRECURSORS TO BORON CARBIDE THIN FILMS, FIBERS AND COMPOSITES Stephen E. Johnson, Xiaoguang Yang, M.F. Hawthorne, Kevin J. Thorne, Haixing Zheng, and John D. Mackenzie	833
BORON CARBIDE NITRIDE DERIVED FROM AMINE-BORANES Jochim Bill and Ralf Riedel	839
POLYMER PRECURSORS FOR ALUMINUM NITRIDE CERAMICS James A. Jensen	845
OPTIMIZATION OF ALUMINUM NITRIDE THERMAL CONDUCTIVITY VIA CONTROLLED POWDER PROCESSING Theresa A. Guiton, James E. Volmering, and Kris K. Killinger	851
*ELECTROCHEMICAL SYNTHESIS OF ALUMINUM NITRIDE IN LIQUID AMMONIA ELECTROLYTE SOLUTIONS Travis Wade, Jongman Park, Gene Garza, Claudia B. Ross, Douglas M. Smith, and Richard M. Crooks	857
ELECTROCHEMICALLY PREPARED POLYMERIC PRECURSORS FOR THE FORMATION OF NON-OXIDE CERAMICS AND COATINGS Ralph Zahneisen and Christian Rüssel	869
ORGANOMETALLIC PRECURSORS TO VANADIUM AND TITANIUM CARBONITRIDE Francois Laurent, Christophe Daures, Lydie Valade, Robert Choukroun, Jean-Pierre Legros, and Patrick Cassoux	875

\*Invited Paper

NEW ROUTES TO GROUP IVA METAL-NITRIDES Chaitanya K. Narula	881
TITANIUM CARBIDE FROM CARBOXYLIC ACID MODIFIED ALKOXIDES Tom Gallo, Carl Greco, Claude Peterson, Frank Cambria, and Johst Burk	887
PREPARATION OF TITANIUM CARBONITRIDE COATINGS BY THE SOL-GEL PROCESS Haixing Zheng, Kris Oka, and John D. Mackenzie	893
XPS STUDY OF THE NITRIDATION PROCESS OF A POLYTITANO- CARBOSILANE INTO Si-Ti-N-O CERAMICS G. Granozzi, A. Glisenti, R. Bertinello, and G.D. Soraru	899
<b>PART VIII: VAPOR PHASE ROUTES TO OXIDE CERAMICS</b>	
*MULTICOMPONENT CERAMIC POWDER GENERATION BY SPRAY PYROLYSIS Shirley W. Lyons, J. Ortega, L.M. Wang, and T.T. Kodas	907
STRUCTURAL AND THERMAL INVESTIGATIONS ON BARIUM, COPPER AND YTTRIUM MOCVD PRECURSORS Alain Gleizes, Dominique Medus, and Sandrine Sans-Lenain	919
ELECTRONIC PROPERTIES OF OMVPE GROWN FILMS OF YBa <sub>2</sub> Cu <sub>3</sub> O <sub>7-x</sub> ON 1" LaAlO <sub>3</sub> SUBSTRATES William S. Rees, Jr., Yusuf S. Hascicek, and Louis R. Testardi	925
REACTION OF BARIUM BIS(β-DIKETONATE) COMPLEXES WITH THE SURFACE OF MAGNESIUM OXIDE R.A. Gardiner, P.S. Kirilin, G.A.M. Hussein, and B.C. Gates	933
OMCVD ELABORATION AND CHARACTERIZATION OF SILICON CARBIDE AND CARBON-SILICON CARBIDE FILMS FROM ORGANOSILICON COMPOUNDS R. Moranco, A. Reynes, M'b. Amjoud, and R. Carles	939
COMPUTATION, VISUALIZATION, AND CHEMISTRY OF ELECTRIC FIELD-ENHANCED PRODUCTION OF CERAMIC PRECURSOR POWDERS Michael T. Harris, Warren G. Sisson, and Osman A. Basaran	945
EFFECT OF DOPANTS IN VAPOR PHASE SYNTHESIS OF TITANIA POWDERS M. Kamal Akhtar, S.E. Pratsinis, and S.V.R. Mastrangelo	951
DEPOSITION OF CERAMIC FILMS BY A NOVEL PULSED-GAS MOCVD TECHNIQUE Kenneth A. Aitchison, James D. Barrie, and Joseph Ciofalo	957
AUTHOR INDEX	963
SUBJECT INDEX	967

\*Invited Paper

# MOLECULAR RECOGNITION ON ACOUSTIC WAVE DEVICES: MODIFIED ZEOLITE-SILICA THIN FILMS WITH TAILORED ADSORPTION PROPERTIES

YONGAN YAN,<sup>a</sup> THOMAS BEIN,<sup>a,\*</sup> KELLY D. BROWN,<sup>b</sup> RAY FORRISTER,<sup>b</sup> and C. JEFFREY BRINKER<sup>c</sup>

<sup>a</sup> Department of Chemistry, Purdue University, West Lafayette, IN 47907, USA

<sup>b</sup> Department of Chemistry, University of New Mexico, Albuquerque, NM 87131, USA

<sup>c</sup> Sandia National Laboratories, P. O. Box 5800, Albuquerque, NM 87185, USA

## ABSTRACT

Microporous thin films composed either of zeolite crystals embedded in sol-gel derived glass or of a molecular coupling layer, zeolite crystals and a porous silica overlayer, were formed on the gold electrodes of Quartz Crystal Microbalances (QCM). The microporosity of the thin films was characterized by *in situ* nitrogen and vapor sorption isotherms. Both preparation methods result in thin films with substantial microporosity. Selective adsorption based on molecular size exclusion from the microporous films could be achieved.

## INTRODUCTION

Growing efforts are being devoted towards the design of chemical microsensors for environmental monitoring and industrial processing [1]. We have recently developed microsensors with molecular sieving functions in chemically selective layers on piezoelectric devices [2,3,4]. The successful design of microporous thin films retaining the molecular sieving capabilities of glass-embedded zeolites requires that several issues be addressed:

- o The glass matrix should not introduce additional, undesired porosity.
- o The glass matrix should not clog the zeolite pores after deposition, i.e., the zeolite porosity should be accessible from the gas phase.
- o The attachment technique should result in a mechanically stable film that provides effective coupling between the zeolite crystals and the oscillating QCM.

*In situ* nitrogen adsorption data of different zeolite-containing glass films were used to explore some of these aspects. In an extension of the glass-based composite approach we have also explored the attachment of zeolite crystals on sensor substrates by molecular means, i.e., by using a bifunctional coupling layer that binds to the substrate as well as to the zeolite crystals. As an example of such a system, we discuss a chemical microsensor with combined molecular sieve and selective surface interactions, based on novel silicalite-silica composite thin films on the active area of QCMs. The function of this sensor will be discussed in the context of selective responses towards ethanol.

In addition to the high sensitivity and selective size exclusion offered by molecular sieve films, the nature of the chemical surface interactions is important. In the thin films described below, interference from water (2.65 Å) which is smaller than ethanol (4.3 Å), could be minimized through hydrophobicity of the molecular sieve and the matrix (silica). The interplay of size exclusion and surface affinity thus provides highly selective adsorption suitable for sensor applications.

## EXPERIMENTAL SECTION

The QCM crystals used in the present study are AT-cut 5-9 MHz piezoelectric resonators, with 0.20 cm<sup>2</sup> gold electrodes deposited on chromium underlayers on opposite sides of the crystal. The sensitivity of a 6 MHz QCM according to the Sauerbrey relationship [5] is 12.3 ng Hz<sup>-1</sup> cm<sup>-2</sup>.

The sol-gel derived, dip-coated composites were prepared from a suspension of silicalite (MFI) and Na-faujasite (FAU) in acid- or base-catalyzed (A2 and B2, respectively) TEOS sols as described previously [2b, 6]. Silicalite is a crystalline molecular sieve of composition  $\text{SiO}_2$  with a pore system of zig-zag channels along *A* (free cross-section ca.  $5.1 \times 5.5 \text{ \AA}$ ), linked by straight channels along *B* ( $5.3 \times 5.6 \text{ \AA}$ ), while FAU is composed of truncated  $\text{Si/Al}$  octahedra (sodalite cages) that form supercages with  $7.5 \text{ \AA}$  circular openings and  $13 \text{ \AA}$  internal diameter, with typical composition  $\text{Na}_{58}\text{Al}_{58}\text{Si}_{134}\text{O}_{384}$  [7].

The preparation of the microporous layer for the ethanol sensor (MFI-EtOH) involved two steps: First, silicalite crystals (about  $3 \mu\text{m}$  diameter) were chemically anchored to the QCM gold electrodes via a thiol-organosilane coupling layer [4]. The silicalite crystals bonded to the QCM electrodes were then further coated with an amorphous, porous silica layer, prepared via sol-gel processing from  $\text{Si}(\text{OEt})_4$  [8], so that stable microporous thin film composites were obtained. Nitrogen sorption at liquid nitrogen temperature on films where the microporosity is presaturated with ethanol revealed a nitrogen monolayer capacity of  $0.0028 \text{ g/(g film)}$ , corresponding to only  $9.8 \text{ m}^2/\text{g}$  external surface area.

The selectivity and sensitivity of the composite film coated QCM devices was determined by measuring the dynamic vapor sorption isotherms in a computer controlled helium vapor flow system. QCM frequency changes of  $0.1 \text{ Hz}$  could be detected with a Keithley 775A frequency counter interfaced to a 386-based personal computer. Equilibrium of the vapor sorption was assumed when the frequency changes were less than  $1.0 \text{ Hz}$  in 30 seconds.

## RESULTS AND DISCUSSION

**Uncoated and glass-coated QCMs.** Nitrogen adsorption isotherms of uncoated QCM crystals are Type II and indicate surfaces with no porosity or with macropores. A polished  $9 \text{ MHz}$  QCM crystal shows a BET surface area of  $2.0 \text{ cm}^2/\text{cm}^2$  and a C constant of 20. This deviation from a perfectly flat surface is attributed to microscopic roughness of the devices. If the crystal is dip-coated with A2 sol and heated in air at  $350^\circ\text{C}$  to result in a coating mass of  $1.55 \mu\text{g}/\text{cm}^2$ , the BET surface area does not increase. However, coating the crystal with a B2-sol derived glass film results in some porosity of the film when heated at the same conditions. The BET surface area increases to  $10 \text{ cm}^2/\text{cm}^2$ .

The conditions of the heat treatment have a profound effect on the porosity of the glass films. Calcination in oxygen at  $450^\circ\text{C}$  further increases the surface area of the films and introduces some microporosity. For instance, if a B2-derived film ( $45 \mu\text{g}/\text{cm}^2$ ) is treated at  $450^\circ\text{C}$ , the BET surface area increases to  $19 \text{ cm}^2/\text{cm}^2$  (corresponding to  $42 \text{ m}^2/\text{g}$ ; derived from the desorption branch), and micropore filling with  $0.019 \text{ g N}_2/\text{g film}$  is observed. In the sorption branch, the micropore filling is  $0.010 \text{ g N}_2/\text{g}$ . The difference between the adsorption and desorption branches found in several isotherms is probably associated with tortuous porosity of diameter close to that of nitrogen, such that hysteresis results.

**Adsorption on Zeolite Sol-Gel Composites.** Silicalite (MFI) and faujasite (NaY) type zeolites were embedded in different sol-gel derived glasses by dip-coating a suspension of the zeolites in the corresponding sol. The microporosity and external surface areas of these films were determined from  $\alpha$ -plots of the nitrogen adsorption isotherms taken on the QCMs.

In general, the isotherms of the zeolite-glass composites show distinct microporosity as indicated by the initial steep rise of the adsorption at very low partial pressures. However, the isotherms differ from ideal Type I (Langmuir) adsorption which would be expected for zeolite crystals. After the initial steep rise the films are not saturated but continue to adsorb nitrogen in a fashion typical for many porous solids with Type IV isotherms. The continued adsorption indicates the presence of meso- and macroporosity that must result from combining the zeolites with the glass matrix.

Figure 1 shows a comparison of adsorption isotherms of silicalite (MFI) embedded in A2 glass and heated to  $350$  and  $450^\circ\text{C}$ . Porosity parameters obtained from these isotherms are listed in Table 1. At about the same total coating weight, the adsorption isotherm resulting from lower temperature heating shows clearly much less adsorption in the micropore region ( $0.015 \text{ g N}_2/\text{g film}$  at  $p/p_0=0.10$ ) than that resulting from high temperature heating ( $0.047 \text{ g N}_2/\text{g film}$  at  $p/p_0=0.10$ ). Even if the desorption branch with the hysteresis is evaluated, higher

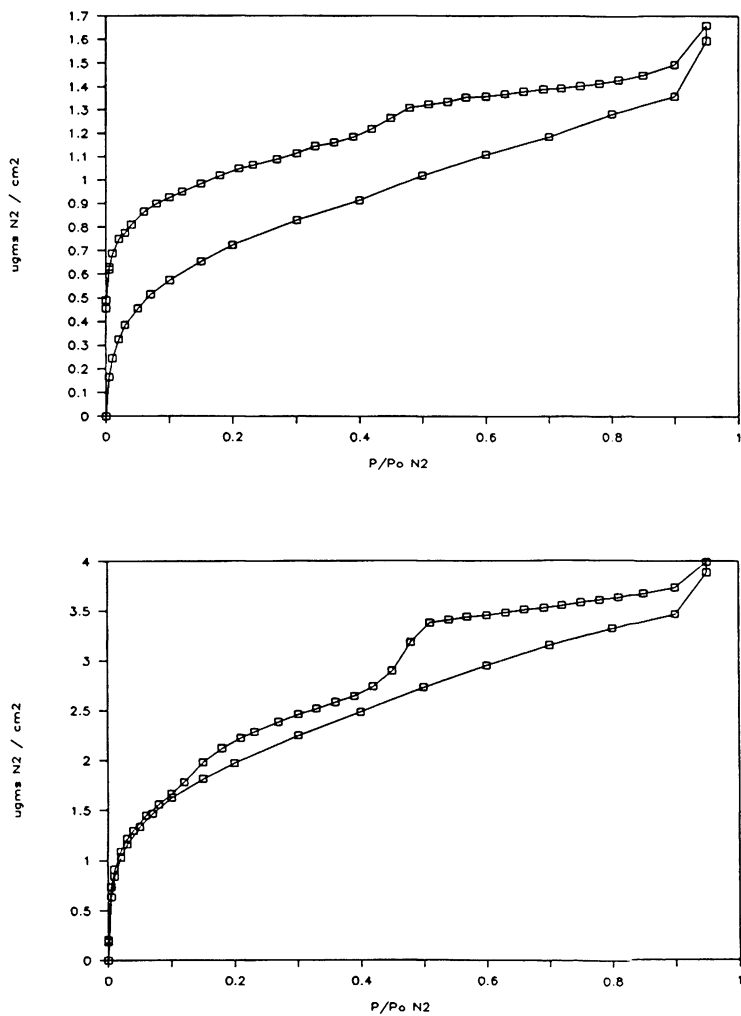


**Figure 1.** Nitrogen adsorption isotherms on silicalite crystals embedded in A2-derived glass films calcined at 350 °C (top), and calcined at 450 °C (bottom).

microporosity results from heating at higher temperature (0.021 vs. 0.014 g N<sub>2</sub>/g). The other important difference between the two isotherms relates to the desorption behavior. After heating at lower temperature, the desorption branch is offset by a strong hysteresis similar to that observed with some of the glass films themselves (see above) which is probably associated with a tortuous pore network of diameters close to that of nitrogen. On heating to 450°C in oxygen, the hysteresis in the low pressure region all but disappears, and some minor hysteresis in the mesopore region remains. Apparently the oxygen treatment removes residual organics from the films such that access to the zeolites is more facile.

The microporosity of these composite films is substantially less than that expected for a film consisting of 100% accessible silicalite (0.17 g N<sub>2</sub>/g). Since the weight fraction of the zeolite in the films is not known, it cannot be determined exactly how much of this decrease in microporosity must be attributed to potential pore clogging, ineffective acoustic coupling, or dilution with the glass film. Previous spectroscopic studies have established that zeolite porosity is accessible in similar films [2b].

**Table 1.** Microporosities and external surface areas of zeolite-glass composite films from nitrogen adsorption isotherms.<sup>a</sup>

Sample	Coating Mass μg/cm <sup>2</sup>	Microporosity g N <sub>2</sub> /g film	External Surface m <sup>2</sup> /g film	Hysteresis at p/p <sub>0</sub> <0.1
MFI-A2-350	39	0.014	36	+
MFI-A2-450	35	0.021	110	-
MFI-B2-350	45	0.029	62	+
MFI-B2-450	34	0.029	138	-
FAU-A2-350	55	0.011	64	-
FAU-A2-450	45	0.017	60	-
FAU-B2-350	51	0.020	35	+
FAU-B2-450	41	0.027	55	-

<sup>a</sup> Evaluated from  $\alpha$ -plots of the desorption branches; when no hysteresis is present (-), the data are similar to those derived from the adsorption branches.

When the silicalite crystals are embedded in a B2-derived glass film, a comparison of the adsorption isotherms obtained after calcination at 350 and 450 °C show very similar trends as with the A2 glass (Table 1). Again, the adsorption isotherm resulting from lower temperature heating shows clearly much less adsorption in the micropore region (0.027 g N<sub>2</sub>/g film at p/p<sub>0</sub>=0.10) than that resulting from high temperature heating (0.059 g N<sub>2</sub>/g film at p/p<sub>0</sub>=0.10). The strong hysteresis disappears only on calcination at 450 °C. The B2-derived glass matrix results in more porous composites than the A2-derived films, as reflected in the higher microporosities and external surface areas, determined at both calcination temperatures. This is consistent with the known behavior of base-catalyzed TEOS sols which retain greater porosity on condensation due to their more compact aggregate structure.

Films derived from faujasite crystals show a different behavior with respect to calcination temperature, compared to silicalite. Figure 2 shows nitrogen sorption isotherms of FAU in A2-derived films. At both temperatures, no hysteresis is observed in the micropore region, but the microporosity still increases on heating to 450 °C, from 0.011 to 0.017 g N<sub>2</sub>/g film. Similarly, little hysteresis is observed if a B2-derived FAU composite is heated to 350 °C, in contrast to the silicalite B2-film. As shown in Table 1, the microporosity of the FAU-B2 films is higher than that of the A2-derived films, but the external surface areas remain similar.

These results suggest that the sols do not affect the access to the larger FAU pores as much as they limit access into silicalite pores at low calcination temperatures where the glass may still contain residual organics. Thus, the adsorption behavior of the FAU films is not much affected by the different calcination treatments.

Relative to the bulk micro-porosity (0.25 g N<sub>2</sub>/g), that of the FAU-containing films is reduced more than that of the MFI films, possibly due to increased penetration of the sol into the larger FAU pores.

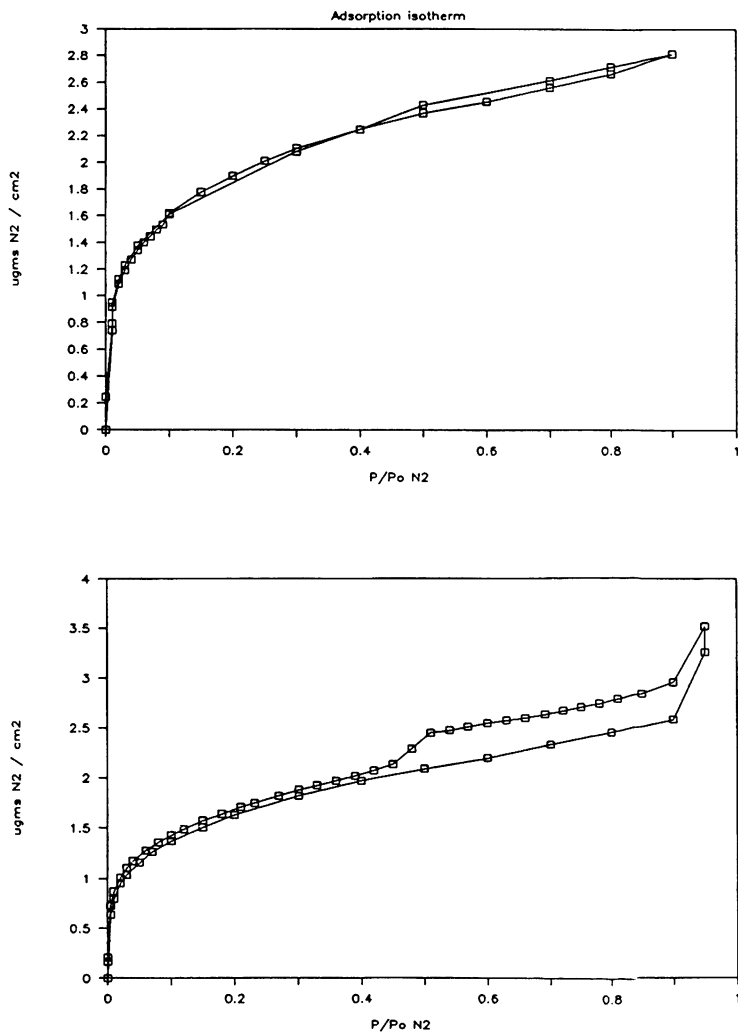


**Figure 2.** Nitrogen adsorption isotherms on faujasite crystals embedded in A2-derived glass films calcined at 350 °C (top), and calcined at 450 °C (bottom).



**Ethanol selectivity.** The selective vapor responses of a QCM coated with the microporous, hydrophobic silicalite composite layer (MFI-EtOH) are illustrated by the sorption of pure vapors of ethanol (ca. 4.3 Å diameter), 2,2,3-trimethylpentane (iso-octane, ca. 6.2 Å) and water (2.65 Å) in the range of 0-2000 parts per million (ppm) in moles (Figure 3). The QCMs were pre-degassed at 170 °C in a helium flow for 20 min. The sorption of ethanol (top curve) shows the largest and fairly linear response as a function of vapor concentration. A 50.4 ppm ethanol vapor concentration results in 0.024 µg sorption per µg coating layer, 309 ppm cause further mass increase to 0.050 µg/µg, and 722 ppm to 0.076 µg/µg, which is about 1000 times higher than the alcohol response of a bare QCM.

In contrast, the response of the microdevice to iso-octane (bottom line) exhibits an almost negligible change with increasing vapor concentration. As the concentration of iso-octane is varied from 200 ppm to 700 ppm, the amount adsorbed changes from 1.66 ng/µg to 1.87 ng/µg, which is a mass increment of only 0.6% of that of alcohol sorption at the same concentrations. The results show that novel sensing layers with highly effective molecular sieving functions and very low external surface areas can be designed. Sorption of the small water molecules (middle line) shows also a small response. Although water sorption slightly increases with increasing concentration (at the two concentrations given above, the capacity is respectively 12.2 and 15.5 ng/µg), it already approaches a rectilinear isotherm at these low concentrations. This behavior differs drastically from the sorption of ethanol.

The microsensor design discussed in this communication shows that highly selective responses can be achieved when microporous adsorption is combined with tailored surface interactions in composite films. Exploration of additional selective interactions in microporous glass composites is in progress.

Funding from the National Science Foundation (Division of Materials Research) and from the Department of Energy (New Mexico WERC program) for this research is gratefully acknowledged.

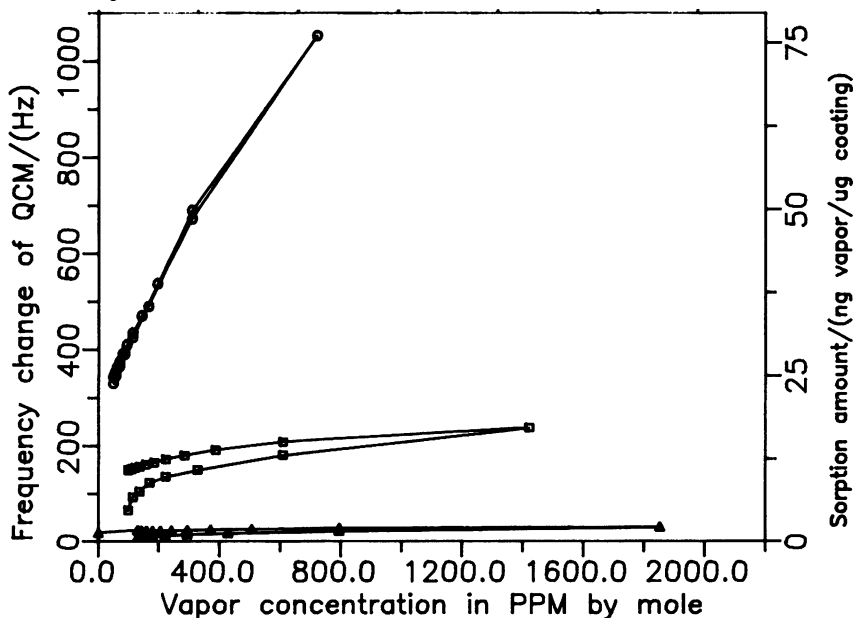


**Figure 3.** Sorption isotherms of ethanol (O), water (II) and isooctane (Δ) on a QCM coated with 168 µg/cm<sup>2</sup> of MFI-EtOH composite at 20 °C.

## REFERENCES

- 1 For recent reviews see: (a) J. Janata, *Anal. Chem.* **62**, 33r (1990). (b) R. C. Hughes, A. J. Ricco, M. A. Butler and S. J. Martin, *Science* **254**, 75 (1991).
- 2 (a) T. Bein, K. Brown, G. C. Frye and C. J. Brinker, U. S. Patent Application 07/580,373, allowed on Jan. 23, 1992. (b) T. Bein, K. Brown, G. C. Frye and C. J. Brinker, *J. Am. Chem. Soc.* **111**, 7640 (1989).
- 3 T. Bein, K. Brown and C. J. Brinker, *Stud. Surf. Sci. Catal.* **49**, P. A. Jacobs, and R. A. Van Santen, Eds.; (Elsevier, Amsterdam, 1989), p. 887.
- 4 Y. Yan and T. Bein, *J. Phys. Chem.*, in press.
- 5  $\Delta f = -2f_0^2 \Delta m A^{-1} (\rho_q \mu_q)^{-1/2}$ , where  $\Delta f$  is the frequency shift,  $f_0$  the parent frequency of the QCM,  $\Delta m$  the mass change in g,  $A$  the piezoelectrically active area in  $\text{cm}^2$ ,  $\rho_q$  the density ( $2.648 \text{ g cm}^{-3}$ ) and  $\mu_q$  the shear modulus ( $2.947 \times 10^{11} \text{ dynes cm}^{-2}$ ) for AT-cut quartz. See: G. Sauerbrey, *Z. Physik* **155**, 206 (1959).
- 6 C. J. Brinker and G. W. Scherer, *Sol-Gel Science*, (Academic Press, San Diego, 1990), p. 110.
- 7 (a) E. M. Flanigen, J. M. Bennett, R. W. Grose, J. P. Cihen, R. L. Patton, R. M. Kirchner and J. V. Smith, *Nature* **271**, 512 (1978). (b) W. M. Meier and D. H. Olson, *Atlas of Zeolite Structure Types*, 2nd Edition, (Butterworths, 1987).
- 8 T. Bein and Y. Yan, U.S. Patent in preparation.